The relation between fatigue crack growth rate and plastic energy dissipation in 7075-T6

Quan, H.; Alderliesten, R. C.

DOI
10.1016/j.engfracmech.2021.107765

Publication date
2021

Document Version
Final published version

Published in
Engineering Fracture Mechanics

Engineering Fracture Mechanics 252 (2021) 107765

Contents lists available at ScienceDirect

Engineering Fracture Mechanics

journal homepage: www.elsevier.com/locate/engfracmech

The relation between fatigue crack growth rate and plastic energy dissipation in 7075-T6

H. Quan *, R.C. Alderliesten

Structural Integrity & Composites, Faculty of Aerospace Engineering, TU Delft, the Netherlands

ARTICLE INFO

Keywords:
Fatigue crack growth
Plastic dissipation
7075-T6

ABSTRACT

Plastic dissipation accompanies fatigue crack growth in ductile materials. Previous studies presented a relation between plastic dissipation (dW/dN) and the fatigue crack growth rate (da/dN), where some researchers assumed a linear relation between both to enable crack growth predictions. To study the validity of this assumption, this paper reports an experimental study on fatigue crack growth in 7075-T6, an alloy widely used in aerospace. The experimental results suggest, however, a nonlinear relation between dW/dN and da/dN in 7075-T6. The value of dW/da, indicating the plastic dissipation per unit fatigue crack growth, is not constant. Hence for 7075-T6 it is concluded that dW/dN cannot be used directly to predict da/dN.

1. Introduction

Fatigue failure is one of the major types of failure in aerospace engineering, and aluminium is one of the most common materials used in aerospace structures. So knowledge on the fatigue behaviour of aluminium alloys is therefore a prerequisite in aerospace to design against fatigue failure. The Paris' relation, which uses similitude parameters coming from linear elastic fracture mechanics (LEFM) such as ΔK or ΔG, is regarded a major method to predict the fatigue crack growth rate (da/dN) in metallic structures.

However, phenomenologically relating ΔK to da/dN does not provide any insight in the role of plasticity, while plasticity influences the fatigue crack rate significantly. The Paris' relation is an engineering approach to predict, using experimental observations, but it does not describe the physics of crack growth properly. So although the Paris' relation is successfully applied in practical engineering, some physics underlying the phenomena of fatigue crack growth is not fully explained.

Elastic-plastic fracture mechanics (EPFM) was proposed to study fatigue crack growth for taking crack tip plasticity into account. Variables such as ΔJ [1–6] or $\Delta CTOD$ [7–9] were used to correlate with da/dN. However, $\Delta CTOD$ is also a phenomenon based variable providing limited information in physics. The application of ΔJ is considered a success, while ΔJ does not indicate well how much plastic work dissipated.

Fortunately, various researchers tried to study the physics of fatigue crack growth from an energy approach and use plastic energy dissipation to predict fatigue crack growth [10–33]. *Weertman* [10] and *Mura* [11] relate the plastic energy to fatigue crack growth, and based on that *Ikeda* [12] proposed an experimental method to measure the plastic energy around crack tip.

Currently, the basis of the energy approach is the relation between plastic energy dissipation per cycle (dW/dN) and fatigue crack growth rate (da/dN). For most of the work [13–30] this relation could be summarized as:

* Corresponding author.
E-mail address: h.quan@tudelft.nl (H. Quan).

https://doi.org/10.1016/j.engfracmech.2021.107765
Received 29 November 2020; Received in revised form 8 April 2021; Accepted 26 April 2021
Available online 2 May 2021

Nomenclature

a	Crack length
A	Fit parameter in Eq. (4)
a_{EXP}	Real crack tip location in experiment
a_{FEA}	Assumed crack tip location in simulation
b	Fit parameter in Eq. (4)
C	Fit parameter in Paris relation
D	Fit parameter in Eq. (5)
da/dN	Fatigue crack growth rate
dW/da	The plastic energy dissipated per unit fatigue crack propagation
dW/dN	The plastic energy dissipation per cycle
dW_{re}/da	The plastic dissipation only over the reversed plastic zone per unit fatigue crack propagation
dW_{re}/dN	The plastic dissipation only over the reversed plastic zone per cycle
dW_{tot}/da	The total plastic energy dissipated per unit fatigue crack propagation
dW_{tot}/dN	The total plastic energy dissipated per cycle
F	Total force on the specimen during fatigue test
G_c	The static fracture toughness
m	Fit parameter in Paris relation
n	Fit parameter in Eq. (5)
δ_{EXP}	Real displacement of reference point in experiment
δ_{far}	Far field displacement on specimen
δ_{FEA}	The simulation results of displacement of reference point
δ_{local}	Local displacement around the crack tip
$\Delta CTOD$	Crack tip opening displacement range
ΔG	Energy release rate range
ΔJ	J- integral range
ΔK	Stress intensity factor range

$$\frac{dW}{dN} = \frac{dW}{da}\frac{da}{dN} \tag{1}$$

Here, dW/da means the plastic energy dissipated per unit fatigue crack propagation. The differences between these studies are in the definitions of the variables in the equation (mainly dW/dN and dW/da), and in the methods to obtain values for these variables. Two forms of dW/dN were often used in research: the total plastic energy dissipated per cycle (dW_{tot}/dN) and the plastic dissipation only over the reversed plastic zone per cycle (dW_{re}/dN).

For example, *Smith* [13], *Klingbeil et al.* [14–18], and *Karlsson et al.* [19–25] performed numerical studies on using the plastic dissipation to predict the fatigue crack growth rate, while *Ranganathan et al.* [26–29] and *Gwider* [30] performed experimental studies on the relation between da/dN and the total energy dissipation.

Among the numerical studies [13–25], Smith [13] proposed a linear relation between da/dN and the total energy dissipated per cycle (dW_{tot}/dN) to simulate the fatigue crack growth of 304 stainless steel with that he considered dW_{tot}/da a material property. Meanwhile, *Klingbeil et al.* [14–18] and *Karlsson et al.* [19–25] used the plastic dissipation only over the reversed plastic zone (dW_{re}/dN) to predict da/dN, but with some differences between their work. *Klingbeil et al.* [14–18] proposed a linear relation between da/dN and the plastic dissipation over the reversed plastic zone per cycle dW_{re}/dN, and claimed that dW_{re}/da is a material property and its value should be equal to the static fracture toughness G_c. While *Karlsson et al.* [19–25] related da/dN with the plastic dissipation in a plastic domain fully enclosing the reversed plastic zone ahead of the crack tip $d\widetilde{W}_{re}/dN$, which is represented by but not totally the same as dW_{re}/dN. In their work, $d\widetilde{W}_{re}/da$ is considered as a material property with its value is nearly constant, but not necessarily equal to G_c.

On the other hand, *Ranganathan et al.* [26–29] and *Gwider* [30] performed experimental studies on the relation between da/dN and dW_{tot}/dN. The total energy dissipation was measured by the load-displacement hysteresis. A nonlinear relation between da/dN and dW_{tot}/dN was observed in the experiments, implying that the value of corresponding dW_{tot}/da is not constant.

Some more studies looked at plastic energy dissipation during fatigue crack growth. For example, *Besel* and *Breitbarth* [31,32] measured the plastic energy dissipation during fatigue crack growth in AA2024-T3 by applying the displacement fields around the crack tip measured with digital image correlation (DIC) as a boundary condition to finite element model. Although they provided with this a method to measure plastic dissipation, they did not present the relation between plastic dissipation and crack growth. *Zheng* [33] simulated fatigue crack growth using the plastic energy density at a critical distance ahead of the crack tip. A relation between da/dN and plastic energy density at a given location is phenomenologically assumed, without addressing the underlying physics.

Besides, it is worth mentioning that the thermography method is a popular approach to study energy dissipation during fatigue crack growth with the help of infrared measurement devices. Different thermal variables were proposed to study fatigue crack growth. For example, *Meneghetti et al.* [34–36] evaluated averaged heat energy inside a volume around crack tip experimentally using infrared

camera, and successfully correlated it to fatigue crack growth data. Palumbo [37] studied the heat dissipated in cyclic plastic zone, and a fourth power dependence of heat dissipated and stress intensity factor was found. *Vshivkov* and *Plekhov et al.* [38–40] studied the relation of the heat flux on da/dN which showed two stages of different properties in fatigue experiments. *Hajshirmohammadi* [41] used entropy flow in plastic zone as a parameter to predict da/dN value. However, the assumption that almost all deformation energy dissipates into heat is proper only in limited cases [38]. So the heat dissipated cannot always fully represent plastic energy and the quantitative relation between plastic energy and the thermal variables proposed is not always clear.

From the review, it could be seen that lots of efforts aimed at establishing a model for predicting da/dN based on the total plastic dissipation dW_{tot}/dN [13,26–30] or the plastic dissipation in the reversed plastic zone dW_{re}/dN [14–25]. Among those, the studies [13–25] effectively presented a scientific hypotheses on a linear relationship between da/dN and dW/dN with a nearly constant dW/da. To question this hypothesis, the current paper reports a combined experimental-numerical study on fatigue crack growth in the typical aluminium 7075-T6 alloy. To verify or falsify the hypothesis on the relationship between dW/dN and da/dN, two questions had to be answered:

1. Do da/dN and dW/dN relate linearly (for both dW_{tot}/dN and dW_{re}/dN) during fatigue crack growth?
2. Does the relation between da/dN and dW/dN (for both dW_{tot}/dN and dW_{re}/dN) remain the same at different stress ratios?

2. Details for fatigue experiments

2.1. Fatigue experiments set-up and test procedure

Eleven centre-crack tension specimens were tested all made from 2 different 7075-T6 plates. Each test was performed at a different maximum stress and stress ratio, the test matrix shown in the Table 1.

The geometry of the specimens is illustrated in Fig. 1. The thickness of the specimens is 3.2 mm. One side of the specimen was painted with a speckle pattern for measuring the strain and displacement fields with DIC method, while the other side of the specimen was for the visual measurement of the fatigue crack length. The initial cracks were made in three steps. First, a 3 mm diameter hole was drilled at the centre of the specimen. Then a small notch of about 2 mm was cut carefully with a jigsaw at both sides of the hole. Finally, fatigue cracks were produced with fatigue precracking until the half crack lengths exceeded 6 mm. After that, the fatigue experiment started.

The fatigue experiments were force-controlled with an MTS 250KkN fatigue machine. The set-up is illustrated in Fig. 2a. During the fatigue experiments, the fatigue crack length was visually measured at Side B of the specimen, with the drilled hole in the centre, as shown in Fig. 2b. The left side crack length was closely the same to the right side crack length during fatigue test. Camera α in Table 1 represents one single 4Mpix camera, and Camera β in Table 1 represents a pair of 5Mpix DIC cameras (the DIC data on Side B is for future research and not used in this paper). The resolution of both Camera α and Camera β was not lower than 14 pixel/mm. Meanwhile at the Side A of the specimen, the strain and displacement fields were measured using the DIC method. For that, the Correlated Solutions Vic-3D DIC system with a pair of 80 mm lenses 5Mpix DIC cameras were positioned at the speckle pattern painted side of the specimen to observe the deformations of the specimens. The area for measuring strain and displacement fields was around 35 mm × 28 mm, larger than the biggest plastic zone size measured by DIC (within 7 mm), so the resolution was around 71 pixel/mm.

The fatigue experiments were performed alternating 1000–3000 (based on fatigue life of test specimen) constant amplitude baseline load cycles at a frequency of 10 Hz with a measurement point containing 6 slow cycles. The slow cycles were applied to allow for load-displacement measurements by the fatigue machine, and for taking photos with the cameras on both sides to accommodate the camera system's time to capture. At both the maximum load and minimum load for every slow cycle, the load of the fatigue machine was hold for 1 s for the cameras to take the photos to measure the corresponding displacement fields and crack length.

Table 1
Test matrix.

Specimen number	R	Max stress (MPa)	Aluminium Sheet Number	Measurement on Side A	Measurement on Side B
1	0.1	48.83	1	A pair of DIC cameras	Camera α
2	0.1	48.83	2		Camera β
3	0.1	70.31	2		Camera β
4	0.3	48.83	2		Camera β
5	0.3	48.83	2		Camera β
6	0.3	70.31	2		Camera β
7	0.5	70.31	1		Camera α
8	0.5	70.31	2		Camera β
9	0.5	78.13	2		Camera β
10	0.7	78.13	1		Camera α
11	0.7	78.13	2		Camera β

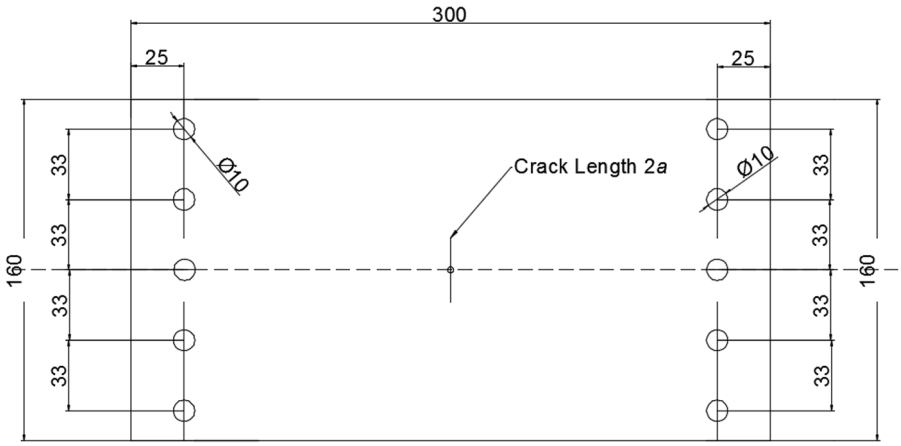

Fig. 1. Specimen geometry.

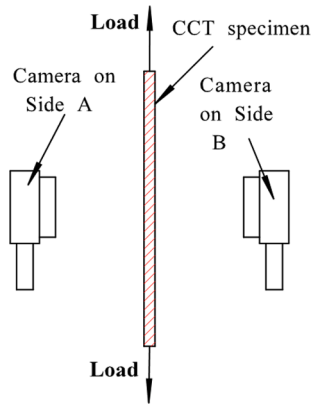

Fig. 2a. Set-up for fatigue test.

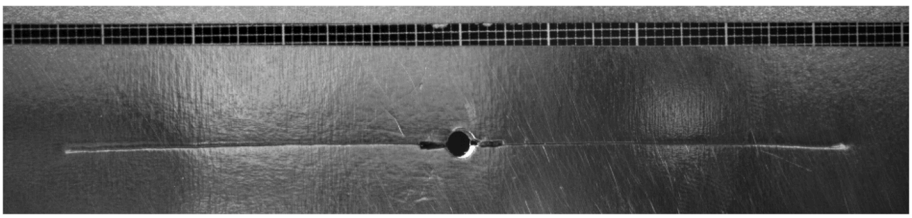

Fig. 2b. Fatigue crack length measurement on side B.

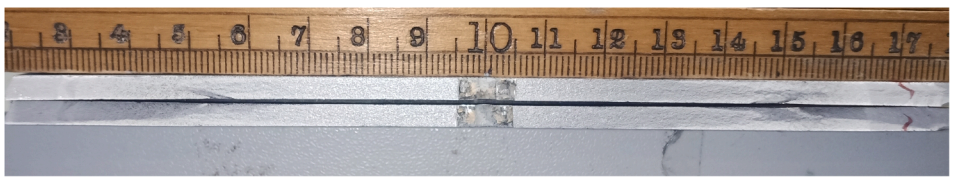

Fig. 2c. Fatigue crack fracture surface.

2.2. Post-processing of experimental data

2.2.1. Obtain fatigue crack growth rate da/dN

The fatigue crack growth rate was calculated from the crack lengths measured from the photos taken in the slow cycles at different numbers of cycles. The 7 point incremental polynomial method recommended in ASTM E647 Standard [42] was used to calculate *da/dN* from crack lengths.

2.2.2. Obtain plastic energy dissipation per cycle dW/dN

Ideally, the plastic energy dissipation per cycle should be calculated by the measured load-displacement hysteresis throughout one entire fatigue cycle:

$$\frac{dW}{dN} = \int F d\delta_{far} \tag{2}$$

where, F is the total far field load on the specimen, and δ_{far} is the far field displacement, whose distribution is nearly uniform in the direction parallel to the direction of the fatigue loading.

However, in reality this is impractical, because the load-displacement hysteresis cannot be observed as the loading-displacement curves during loading and unloading approximately coincide. The plastic dissipation per cycle is too small compared with the change in elastic strain energy during a half load cycle.

Even when local displacement around the crack tip δ_{local} is used instead of the far field displacement, the resolution is insufficient. Since 7075-T6 is not as ductile as other typical aluminium alloys such as 2024-T3, the hysteresis in F-δ_{local} curves for loading and unloading approximately coincide in most cases, because the plastic energy dissipation is very small. Although the F-δ_{local} hysteresis is detectable at high ΔK values under low stress ratio, the integration result of F-δ_{local} hysteresis does not represent the physical total plastic dissipation or plastic dissipation over the reversed plastic zone. Therefore, it is not practical to use the integration of the load-displacement hysteresis loop throughout one entire fatigue cycle to measure the plastic energy dissipation per cycle.

In order to solve this problem, a method based on numerical simulation was utilized to obtain the values of plastic energy dissipation per cycle. The concept is to apply the displacement field measured by DIC on Side A as boundary condition to the finite element model to obtain the plastic dissipation values through simulation. This method is explained hereafter.

2.2.2.1. Apply the experimental displacement to numerical model. The displacement field of the shaded area in Fig. 3 was measured using DIC. Half of this area was simulated in the numerical model, and the displacements measured in the experiment were applied to the numerical model as boundary condition.

Fig. 3 illustrates the concept applying the displacement in FEA simulation using a two dimensional 1/2 model, because for Mode I crack propagation the symmetric constrain could be applied. The height of the FEA model of each specimen was just slightly larger than the maximum size of the plastic area throughout the test to include the whole plastic zone in the model. The width of the FEA model was as long as possible within the experimental measured area, making the plastic dissipation mainly determined by the displacement on the top side.

On the left side of the FEA model both displacements of X and Y directions were applied except for an small area beside the crack surface as shown in Fig. 3. Because the crack damages the speckle pattern on the DIC surface making the image correlation with the reference without crack sometimes impossible, hence it sometimes was impossible to measure the displacement near the crack surface. In addition, the displacement measured by DIC near crack surface is not accurate, because DIC measures the displacement of one point based on a small local neighbourhood area, effectively "smoothening" it by the local neighbourhood area. For a continuum displacement field the error is acceptable, but for the discrete displacement field, for example around the crack surface, the error is unacceptable, as a simple illustration shows in Fig. 4.

The size of the small area without displacement constraint on the left side of the FEA model was around 0.5–1 mm, larger than the

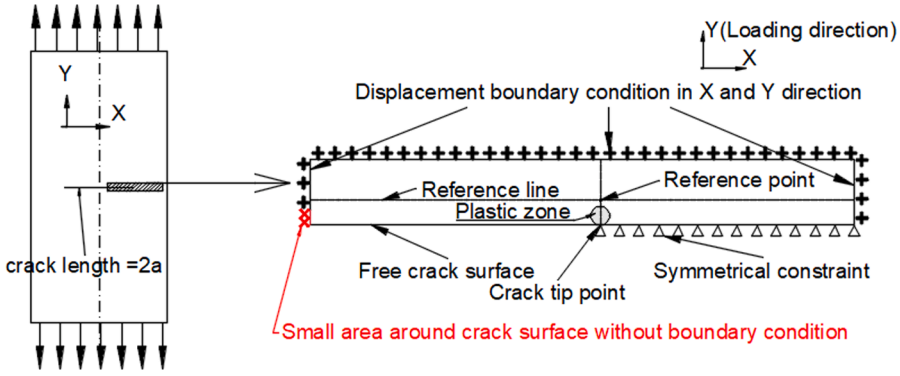

Fig. 3. Displacement measurement area on test specimen (left) and Half FEA model to simulate the displacement measurement area (right).

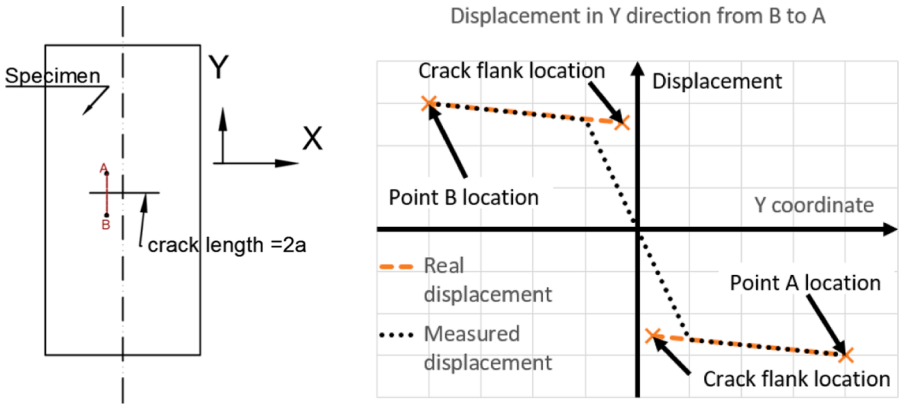

Fig. 4. Measurement of displacement in loading direction around crack surface from Point B to point A.

half size of the neighbourhood area using for DIC measuring displacement, in order to exclude crack surface in the displacement measurement.

The crack surface was regarded as free surface in FEA model and the symmetrical boundary constraint was applied on the remaining part of the bottom side of the model. A rigid line was positioned at the crack surface to consider possible crack closure. The tangential frictionless contact and vertical hard contact were used for contact properties for the case of closure.

The length and width of the specimen were much larger than the thickness, so the specimen plate was considered as plane stress condition. Thus, the displacements in thickness direction were neglected. As a result, the free surface of the specimen was assumed to represent the whole specimen. Hence, the numerical model was considered in plane stress condition and the displacement on the free surface was regarded as the displacement throughout thickness. The simulation is done under small strain condition. The element type used was 4 node reduced integration element with enhanced hourglass control.

The material property of 7075-T6 used is based on the tensile experimental data of 6 specimens shown in figure below. The elasto-plastic model with nonlinear kinematic hardening in ABAQUS was chosen to simulate the material property. The material property in simulation and tensile experimental data are shown in Figs. 5a and 5b. The Poisson ratio is 0.33.

The crack was simulated as stationary crack as in [14,26]. Six fatigue cycles were applied to simulate the six slow cycles in fatigue tests. The first cycle was utilized to generate an initial plastic field to reach a stable cycle afterwards, and then the plastic dissipation per cycle was averaged from 5 cycles afterwards. Each cycle was simulated by first applying the displacement at the maximum load

Fig. 5a. Specimens for tensile test.

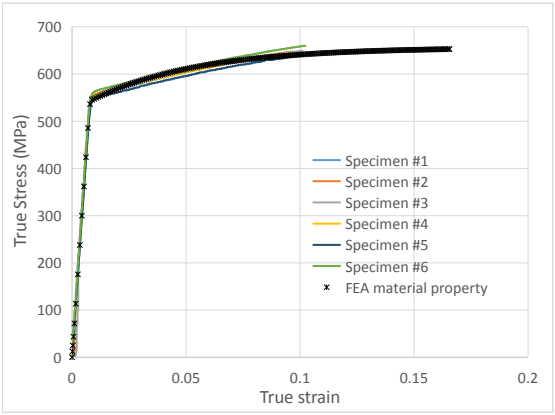

Fig. 5b. The material property in simulation and tensile experimental data.

then applying the displacement at the minimum load. The displacement applied at the maximum load was the average of the experimental measured displacement at the maximum load of the 6 slow cycles. The displacement applied at the minimum load was the average of the experimental measured displacement at the minimum load of the 6 slow cycles.

2.2.2.2. Solution to find the exact crack tip location. Because the exact crack tip location cannot be established with sufficient accuracy in the experiment, an indirect method was adopted in the simulation. By comparing correlating measured DIC displacements with simulated displacements to find the best fit, the crack tip location was determined.

As shown in Fig. 3, there is a reference line, which is 1 mm away from the symmetric surface and crack surface. The displacement of a reference point, which lays at the same x-coordinate with the crack tip point in the reference line as shown in Fig. 3, was used to determine the exact crack tip location as shown in Fig. 6. As shown in Fig. 6, the FEA results of displacement of reference point δ_{FEA} with different assumed crack tip locations a_{FEA} could be obtained numerically. Then the relation between δ_{FEA} and a_{FEA} was obtained as the red interpolation line in Fig. 6. Finally, the X and Y coordinates of the intersection in Fig. 6 of the interpolation line (red) and the experimental displacement field of the reference line (blue line) gave the real crack tip location a_{EXP} and real displacement of reference point δ_{EXP} in the experiments.

2.2.2.3. Summary of the numerical model. The experimentally measured displacement was applied as boundary condition as in Section 2.2.2.1. The exact position of the crack tip was obtained by comparing the displacement from simulations with different crack lengths to the experimentally measured displacement to find the best fit as in Section 2.2.2.2. The method proposed in this paper follows the similar concept to obtain plastic dissipation as presented in [31,32]. The concept is similar to Global-to-Local Modelling. Here, the "global model" is the experimental fatigue specimens, and the "local model" is the FEA model shown in Fig. 7. The displacement measured by DIC is the boundary between the global and local models. The FEA model used in this paper is a local modelling of the real fatigue experiments based on the displacement measurement.

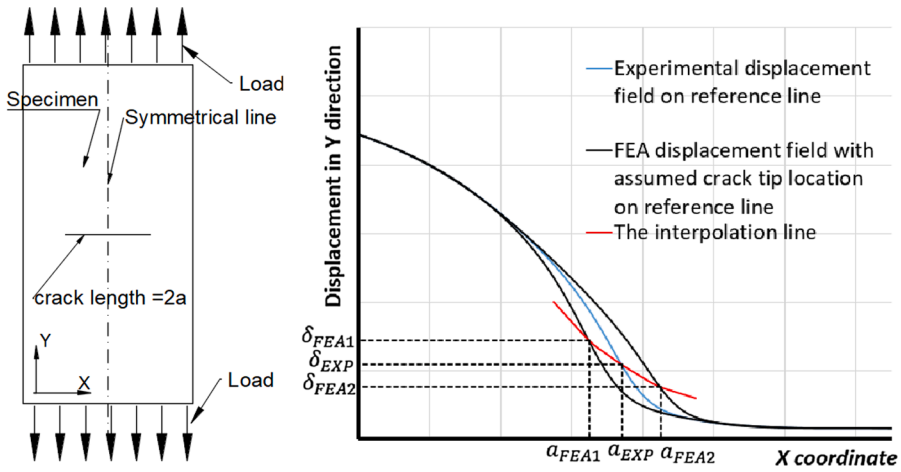

Fig. 6. Method to find crack tip location with displacement.

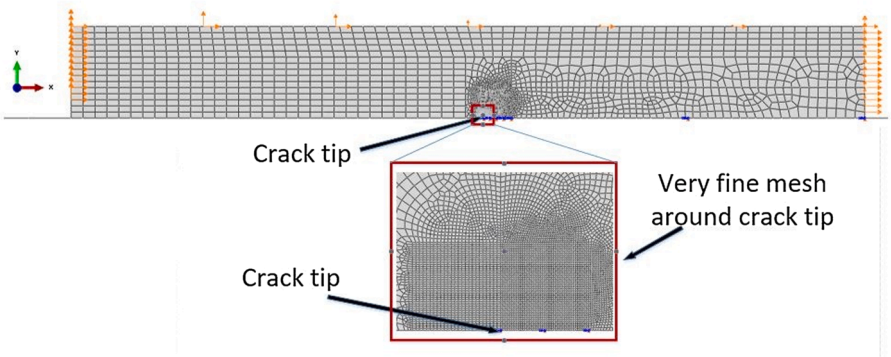

Fig. 7. The FEA model to obtain plastic dissipation.

3. Experimental result

After the fatigue experiments, the values of da/dN and dW/dN were obtained with the methods in 2.2. The results are shown below. First, as the ASTM E647 Standard [42] recommended, the da/dN is plotted against ΔK in Fig. 8. The fatigue crack growth data could be described by the Paris' equation normally:

$$\frac{da}{dN} = C(\Delta K)^m \tag{3}$$

All the parameters in the equations in this paper are fitted with the data in the Paris' region. The parameters in the equation are in Table 2.

Second, after obtaining the plastic dissipation dW/dN with the method proposed in Section 2.2.2, the dW/dN is also plotted against the ΔK in the Figs. 9a and 9b to make it easy for comparing with da/dN afterwards. All the plastic dissipation values shown in this paper are already been normalized on unit thickness unless otherwise specified. The relation between dW/dN and ΔK could be fitted very well in a power law:

$$\frac{dW}{dN} = A(\Delta K)^b \tag{4}$$

Here the parameters in the equation are in Table 3.

The values of the total plastic energy and the energy over the reversed plastic zone are close, because the energy over the reversed plastic zone occupies the major part of the total plastic energy. Especially for $R = 0.1$ and 0.3, the energy over the reversed plastic zone is over 90% of the total plastic energy. More discussion on experimental data is presented in the next section.

4. Discussion

4.1. The relation between plastic energy dissipation and fatigue crack growth rate

In order to answer the question asked previously in this paper on the relation between da/dN and dW/dN, the da/dN and plastic dissipation are plotted together into the same figure to see the trend as shown in Figs. 10a and 10b below.

The relation between dW/dN and da/dN can be fitted to a power law:

$$\frac{da}{dN} = D\left(\frac{dW}{dN}\right)^n \tag{5}$$

with the parameters in the equation below in Table 4.

If the relation between dW/dN and da/dN is linear and the value of dW/da constant, then the curve of dW/dN and da/dN can be fitted with a power law with exponent 1. However, from the data above it can be concluded that the relation for all stress ratios shows a strong nonlinear trend. Thus the relation between dW/dN and da/dN is nonlinear, and the value of dW/da is not constant. Meanwhile, for $R = 0.1$,0.3 and 0.5 the trend is more nonlinear than $R = 0.7$, expressing the value of dW/da changes differently among different stress ratios.

The nonlinearity in dW/dN - da/dN data depends on the values of m in Eq. (3) and b in Eq. (4). With R increasing, the value of m becomes closer to b, meaning less nonlinearity in dW/dN - da/dN data. The value of b is around 4 throughout the test while m changes from 2.2 at $R = 0.1$ to 3.5 at $R = 0.7$. Hence, the nonlinearity in dW/dN - da/dN data corresponds to a slope change of the $da/dN - \Delta K$ curve on log–log scales. Similar phenomena are also reported in [43], with the slope of $da/dN - \Delta K$ curves on log–log scale changes with stress ratio for both 9021-T4 and 7090-T6 alloy, which is attributed to the changing crack growth mechanisms in [43]. Similarly, the decreasing nonlinearity with stress ratio in current dW/dN - da/dN data could be also explained with the change in fatigue crack growth mechanics.

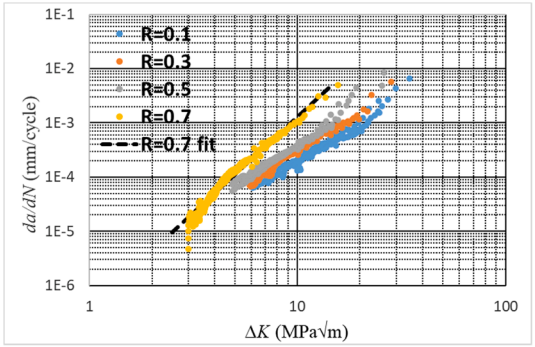

Fig. 8. Fatigue crack growth rate.

Table 2
The parameters in Paris' equation.

R	C	m
0.1	1.172×10^{-6}	2.211
0.3	1.061×10^{-6}	2.445
0.5	1.402×10^{-6}	2.427
0.7	3.721×10^{-7}	3.545

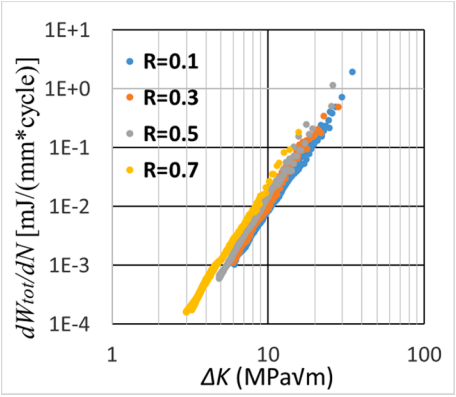

Fig. 9a. Total plastic dissipation per cycle in unit thickness against ΔK.

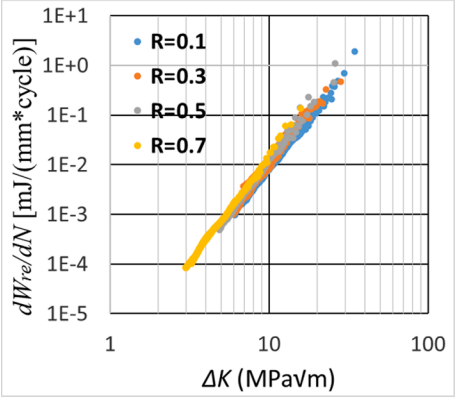

Fig. 9b. Plastic dissipation per cycle in reversed plastic zone in unit thickness against ΔK.

Table 3
The parameters in Eq. (4).

R	Total plastic dissipation		Plastic dissipation in reversed plastic zone	
	A	b	A	b
0.1	8.384×10^{-7}	4.027	7.712×10^{-7}	4.041
0.3	6.947×10^{-7}	4.236	5.960×10^{-7}	4.263
0.5	8.237×10^{-7}	4.236	6.598×10^{-7}	4.247
0.7	1.706×10^{-6}	4.125	8.326×10^{-7}	4.239

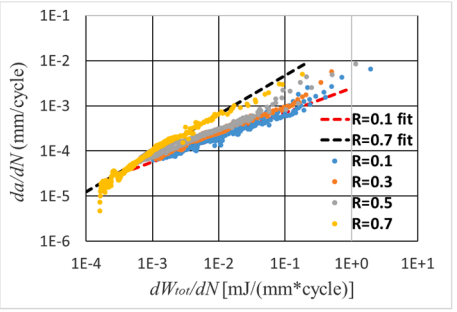

Fig. 10a. Total plastic dissipation per cycle against fatigue crack growth rate.

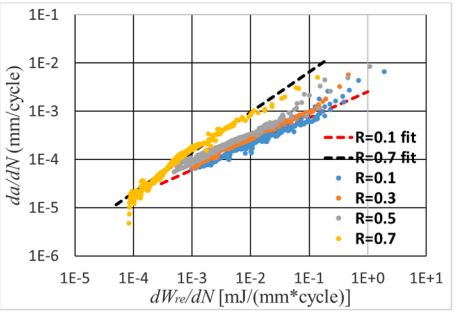

Fig. 10b. Plastic dissipation in reversed plastic zone per cycle against fatigue crack growth rate.

Table 4
The parameters in Eq. (5).

R	Total plastic dissipation		Plastic dissipation in reversed plastic zone	
	D	n	D	n
0.1	0.002494	0.5445	0.002543	0.5424
0.3	0.003752	0.5741	0.003885	0.5702
0.5	0.004266	0.5717	0.004752	0.5705
0.7	0.03363	0.8591	0.04463	0.8346

4.2. The value of dW/da

The value of dW/da was calculated from dW/dN in Eq. (1). Therefore, the reason for the slope change of dW/da – da/dN curves on log–log scale with different R in Figs. 11a and 11b should be the same as the reason for the slope change of dW/dN – da/dN curves on log–log scale, which is the change in fatigue crack growth mechanics.

The value for dW/da at $R = 0.7$ first decreases with increasing da/dN. Then it holds steady for a certain period and finally gradually rises. The descending part of $R = 0.7$ coming from the nonlinear part of the da/dN-ΔK curve, expresses obvious nonlinear trend of $R =$ 0.7 curve.

The trend for $R = 0.7$ is similar to the trend of 7075-T7351 in [30], as shown in Fig. 12. The dW_{tot}/da values of both 7075-T6 in this paper and 7075-T7351 in [30] are almost constant in the range of 2×10^{-5}mm/cycle $< da/dN < 10^{-3}$mm/cycle. The dW_{tot}/da values for 7075-T7351 are higher, because the range of ΔK for 7075-T7351 (9-32MPa$\sqrt{\text{m}}$) in the range 2×10^{-5}mm/cycle $< da/dN <$

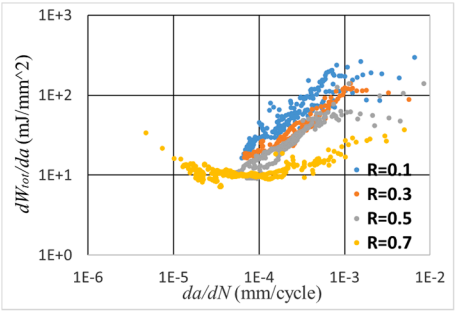

Fig. 11a. dW_{tot}/da against da/dN for four different stress ratios.

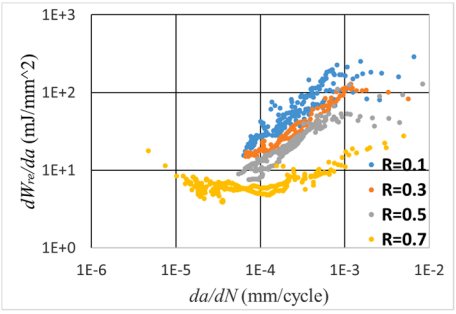

Fig. 11b. dW_{re}/da against da/dN for four different stress ratios.

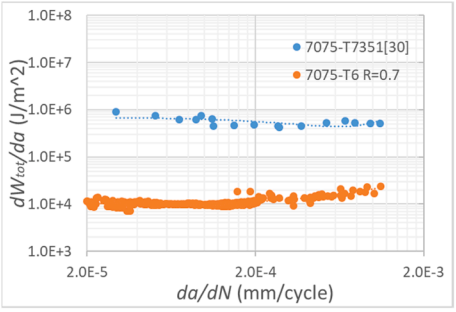

Fig. 12. Comparison of current dW/da data with data for 7075-T7351 from [30]

10^{-3}mm/cycle is much larger than the range of ΔK for 7075-T6 (3.3-10MPa$\sqrt{m}$), resulting in more plastic dissipation at the same da/dN for 7075-T7351.

The dW/da values at $da/dN = 3 \times 10^{-7}$m/cycle for 7050-T76 and 7050-T4 were reported in [12], which are compared with current result in Table 5. All the results have a similar magnitude, providing confidence in the experimental results generated in the current study.

Figs. 11a and 11b shows that the value of dW/da at $R = 0.1$, 0.3 and 0.5 increases, except for the fatigue crack growth final stage when da/dN increases rapidly, and the same observation for $R = 0.1$, 0.3 and 0.5 can be made when plotting dW/da against ΔK, as shown in Fig. 13. Additionally, it is worth mentioning that in Fig. 13(a) the relation between dW_{tot}/da and ΔK falls almost into the same scatter band regardless of the different stress ratios.

Table 5
Comparison of current data with data from [12]

	dW/da(J/m^2)	R
7050-T76 [12]	6.3*10^4	0.05
7050-T4 [12]	5.4*10^4	0.05
7075-T6	6.8*10^4	0.1

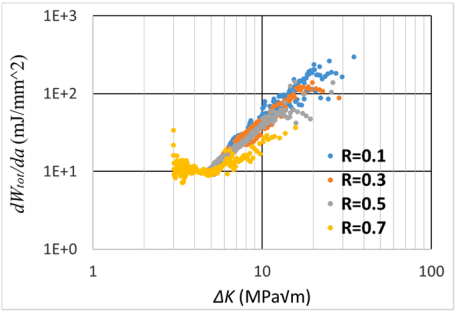

Fig. 13a. dW_{tot}/da against ΔK for four different stress ratios.

To explain the behaviour shown in Figs. 11a and 11b and 13a and 13b, one should put dW/da and ΔK or da/dN in one equation. Here this equation is derived from Eqs. (3) and (4). Table 3 reveals that the dW/dN and ΔK can be described with a power law and the exponent b is approximately 4 in Eq. (4). This result agrees with the simulation results from [14], the analytical solution of plastic energy dissipation in [26,44] and the heat dissipated measured experimentally in [37]. Therefore, a power law with exponent b equal to 4 can be a good approximation to estimate the plastic dissipation as function of the stress intensity factor. Then here 4 could be used to replace the exponent b in Eq. (4). Dividing Eq. (4) by Eq. (3) yields:

$$\frac{dW}{da} = \frac{A}{C}(\Delta K)^{4-m} \tag{6}$$

The equation shows the overall trend in Paris' region of how dW/da changes with ΔK. Similarly dW/da changes with da/dN because da/dN increases monotonically with ΔK increasing. If the exponent m in the Paris' equation is lower than 4, the value of dW/da will rise with da/dN increasing. But if the exponent m is larger than 4, the value of dW/da will decrease with da/dN increasing. If the exponent m is close to 4, it could then be expected the value of dW/da will remain generally stable with da/dN increasing.

In the cases of $R = 0.1$, 0.3 and 0.5, dW/da is increasing, while for $R = 0.7$, dW/da decreases first and after a transition it increases. The reason is that in the cases of $R = 0.1$, 0.3 and 0.5, the exponent m is about 2.4, which is far less than 4. However, the exponent m of $R = 0.7$ is to 3.545, which is slightly lower than 4. Therefore, it should not be surprising that the dW/da first almost levels off in the Paris' region although the overall trend is going up for $R = 0.7$. Additionally, for $R = 0.7$, When $\Delta K < 3.5\text{MPa}\sqrt{\text{m}}$and $da/dN < 3 \times 10^{-5}$mm/cycle, the dW/da value decreases, because da/dN grows rapidly with ΔK, which is not described in Paris' equation, but dW/dN grows steadily with ΔK. However, for the cases of $R = 0.1$, 0.3 and 0.5, the data in this part is not included, so the deceasing trend at the beginning cannot be observed.

Above all, it could be concluded that the dW/da is not a constant for 7075-T6. In this way, the assumption of linear relation between da/dN and dW/dN is falsified. Therefore, it is not appropriate to use either the plastic dissipation or the plastic dissipation in reversed plastic zone to predict the fatigue crack growth rate of 7075-T6. While the plastic dissipation could be a good method to predict the fatigue crack growth when the exponent m in Paris' equation is close to 4. Moreover, the relation between dW/dN and da/dN is different for different stress ratios.

4.3. Limitation of current work

There are still some limitations to the current work. The major limitation comes from the plastic dissipation obtained through FEA with the experimental displacement as boundary condition rather than being measured directly from the fatigue experiment. The FEA model used in the simulation is strictly not reflecting the real tests.

First in the simulation a pure Mode I case is assumed. So half the model is simulated with symmetrical boundary conditions.

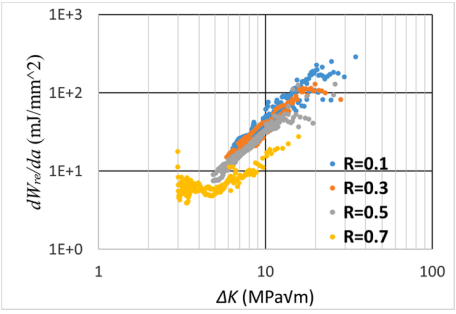

Fig. 13b. dW_{re}/da against ΔK for four different stress ratios.

Nevertheless, in reality the fatigue crack is not in pure Mode I, because the crack surface is not smooth instead of being flat as assumed in FEA. For example, the current study ignores the effect of shear lips, which will make the plastic dissipation larger than plastic dissipation with flat fracture surface assumed in simulation. However, Fig. 2c shows that the majority of the fatigue crack surface is very flat, and obvious shear lips happens only at high ΔK. Therefore, the effect of shear lips is limited in current test, because most of the results have little change and the overall trend remains the same. However, the dW/dN and dW/da should be larger in the last several measuring points in high ΔK region.

Then in the simulation, a plane stress condition is assumed, meaning a uniform distribution throughout the thickness direction and the influence of thickness is neglected. Nonetheless, in reality, it is a 3D case. At the mid-plane of the specimen, it is more like plane strain condition. However, in the simulation the plane stress condition is used for simulating the whole thickness and in experiments the displacement field on the surface is assumed representing the whole specimen.

Finally, the crack is simulated with a stationary crack. In this way, the effect of the residual plastic wake behind the crack tip is ignored, and the influence of fatigue crack growth is also neglected.

Therefore, in the future, a more detailed numerical 3D analysis could shed light on these limitations, or a better method to directly obtain the plastic dissipation from experiments is needed.

5. Conclusion

An experimental study is reported in this paper to investigate the relation between plastic energy dissipation and the fatigue crack growth rate in 7075-T6 at $R = 0.1$, 0.3, 0.5 and 0.7. It is concluded that both the total plastic dissipation per cycle and the plastic dissipation in the reversed plastic zone show a nonlinear relation with da/dN for 7075-T6. Hence, for the tested range in da/dN between 10^{-5} and 10^{-2} mm/cycle, the value of dW/da for 7075-T6 is not constant, implying that the plastic dissipation cannot be used to predict the fatigue crack growth rate directly for 7075-T6. In this case, the assumption of linear relation between da/dN and dW/dN is falsified. Moreover, the relation between dW/dN and da/dN is different for different stress ratios

However, when the exponent in the Paris' equation is close to 4, the plastic dissipation could be regarded as approximately linearly related to the fatigue crack growth rate. If that condition is met, the plastic dissipation might be a good method to predict fatigue crack growth rate.

Declaration of Competing Interest

The authors declare that they have no known competing financial interests or personal relationships that could have appeared to influence the work reported in this paper.

References

[1] Azmi MS Muhamad, et al. On the ΔJ-integral to characterize elastic-plastic fatigue crack growth. Engng Fract Mech 2017;176:300–7.
[2] Al-Sugair Faisal H. Explicit cyclic J-integral expressions for low-cycle fatigue modeling of plane stress crack problems. Engng Fract Mech 1992;43(3):313–20.
[3] Chow CL, Lu TJ. Cyclic J-integral in relation to fatigue crack initiation and propagation. Engng Fract Mech 1991;39(1):1–20.
[4] Banks-Sills Leslie, Volpert Yehuda. Application of the cyclic J-integral to fatigue crack propagation of Al 2024–T351. Engng Fract Mech 1991;40(2):355–70.
[5] Srivastava YP, Garg SBL. Study on modified J-integral range and its correlation with fatigue crack growth. Engng Fract Mech 1988;30(2):119–33.
[6] Wang Jie, et al. Numerical assessment of cyclic J-integral△ J for predicting fatigue crack growth rate. Engng Fract Mech 2019;205:455–69.
[7] Vasco-Olmo JM, et al. Characterisation of fatigue crack growth using digital image correlation measurements of plastic CTOD. Theor Appl Fract Mech 2019;101:332–41.
[8] Antunes FV, et al. Fatigue crack growth versus plastic CTOD in the 304L stainless steel. Engng Fract Mech 2019;214:487–503.
[9] James MN, et al. Characterisation of fatigue crack growth using the CJP model of crack tip fields or plastic CTOD. Procedia Struct Integrity 2019;23:613–9.
[10] Weertman J. Theory of fatigue crack growth based on a BCS crack theory with work hardening. Int J Fract 1973;9:125–31.
[11] Mura T, Lin CT. Theory of fatigue crack growth for work hardening materials. Int J Fract 1974;10(2):284–7.
[12] Ikeda S, Izumi Y, Fine ME. Plastic work during fatigue crack propagation in a high strength low alloy steel and in 7050 Al alloy. Engng Fract Mech 1977;9:123–36.
[13] Smith KV. Application of the dissipated energy criterion to predict fatigue crack growth of Type 304 stainless steel following a tensile overload. Engng Fract Mech 2011;78(18):3183–95.
[14] Klingbeil NW. A total dissipated energy theory of fatigue crack growth in ductile solids. Int J Fatigue 2003;25(2):117–28.
[15] Daily JS, Klingbeil NW. Plastic dissipation in fatigue crack growth under mixed-mode loading. Int J Fatigue 2004;26(7):727–38.
[16] Baudendistel CM, Klingbeil NW. Effect of a graded layer on the plastic dissipation in mixed-mode fatigue crack growth along plastically mismatched interfaces. Int J Fatigue 2013;51:96–104.
[17] Daily JS, Klingbeil NW. Plastic dissipation in mixed-mode fatigue crack growth along plastically mismatched interfaces. Int J Fatigue 2006;28(12):1725–38.
[18] Daily JS, Klingbeil NW. Plastic dissipation energy at a bimaterial crack tip under cyclic loading. Int J Fatigue 2010;32(10):1710–23.
[19] Cojocaru D, Karlsson AM. Assessing plastically dissipated energy as a condition for fatigue crack growth. Int J Fatigue 2009;31(7):1154–62.
[20] Nittur PG, Karlsson AM, Carlsson LA. Numerical evaluation of Paris-regime crack growth rate based on plastically dissipated energy. Engng Fract Mech 2014;124:155–66.
[21] Ding G, Karlsson AM, Santare MH. Numerical evaluation of fatigue crack growth in polymers based on plastically dissipated energy. Int J Fatigue 2017;94:89–96.
[22] Cojocaru D, Karlsson AM. An object-oriented approach for modeling and simulation of crack growth in cyclically loaded structures. Adv Engng Softw 2008;39(12):995–1009.
[23] Moslemian R, Karlsson AM, Berggreen C. Accelerated fatigue crack growth simulation in a bimaterial interface. Int J Fatigue 2011;33(12):1526–32.
[24] Nittur PG, Karlsson AM, Carlsson LA. Implementation of a plastically dissipated energy criterion for three dimensional modeling of fatigue crack growth. Int J Fatigue 2013;54:47–55.
[25] Ding G, Santare MH, Karlsson AM, Kusoglu A. Numerical evaluation of crack growth in polymer electrolyte fuel cell membranes based on plastically dissipated energy. J Power Sources 2016;316:114–23.
[26] Ranganathan N, Chalon F, Méo S. Some aspects of the energy based approach to fatigue crack propagation. Int J Fatigue 2008;30(10–11):1921–9.

[27] Mazari M, Bouchouicha B, Zemri M, Benguediab M, Ranganathan N. Fatigue crack propagation analyses based on plastic energy approach. Comput Mater Sci 2008;41(3):344–9.
[28] Ranganathan N, Desforges JR. Equivalent constant amplitude concepts examined under fatigue crack propagation by block loading. Fatigue Fract Engng Mater Struct 1996;19(8):997–1008.
[29] Ranganathan N, Jendoubi K, Benguediab M, Petit J. Effect of R ratio and ΔK level on the hysteretic energy dissipated during fatigue crack propagation. Scr Metall 1987;21(8):1045–9.
[30] Gwider A. Contribution to the Applicability of Energy Based concepts for Fatigue Crack Propagation. Thesis University of Tours; 2019.
[31] Breitbarth E, Besel M. Energy based analysis of crack tip plastic zone of AA2024-T3 under cyclic loading. Int J Fatigue 2017;100:263–73.
[32] Besel M, Breitbarth E. Advanced analysis of crack tip plastic zone under cyclic loading. Int J Fatigue 2016;93:92–108.
[33] Zheng X, Cui H, Su X, Engler-Pinto Jr CC, Wen W. Numerical modeling of fatigue crack propagation based on the theory of critical distances. Engng Fract Mech 2013;114:151–65.
[34] Meneghetti G, Ricotta M. Evaluating the heat energy dissipated in a small volume surrounding the tip of a fatigue crack. Int J Fatigue 2016;92:605–15.
[35] Meneghetti G, Ricotta M. A heat energy dissipation approach to elastic-plastic fatigue crack propagation. Theor Appl Fract Mech 2020;105:102405.
[36] Meneghetti G, Ricotta M. The heat energy dissipated in the material structural volume to correlate the fatigue crack growth rate in stainless steel specimens. Int J Fatigue 2018;115:107–19.
[37] Palumbo D, et al. Damage monitoring in fracture mechanics by evaluation of the heat dissipated in the cyclic plastic zone ahead of the crack tip with thermal measurements. Engng Fract Mech 2017;181:65–76.
[38] Vshivkov A, et al. The experimental and theoretical study of heat dissipation at fatigue crack tip under biaxial loading. Theor Appl Fract Mech 2019;103:102308.
[39] Plekhov O, et al. The heat dissipation at fatigue crack tip under mix mode loading. Procedia Struct Integrity 2018;13:1209–14.
[40] Vshivkov AN, et al. The study of a fatigue crack propagation in titanium Grade 2 using analysis of energy dissipation and acoustic emission data. Engng Fract Mech 2019;210:312–9.
[41] Hajshirmohammadi B, Khonsari MM. On the entropy of fatigue crack propagation. Int J Fatigue 2020;133:105413.
[42] ASTM. E647 Standard Test Method for Measurement of Fatigue Crack Growth Rates. West Conshohocken, PA: ASTM International; 2015.
[43] Vasudevan AK, Sadananda K. Classification of environmentally assisted fatigue crack growth behavior. Int J Fatigue 2009;31(11-12):1696–708.
[44] Khelil F, Aour B, Belhouari M, Benseddiq N. Modeling of fatigue crack propagation in aluminum alloys using an energy based approach. Engng Technol Appl Sci Res 2013;3(4):488–96.